2019

Simulation Study of the Emittance Measurements in Magnetized Electron Beam

S.A.K. Wijethunga
Old Dominion University

J. Benesch

Jean R. Delayen
Old Dominion University, jdelayen@odu.edu

F. E. Hannon

Geoffrey A. Krafft
Old Dominion University, gkrafft@odu.edu

See next page for additional authors

Original Publication Citation

Wijethunga, S. A. K., Benesch, J., Delayen, J. R., Hannon, F. E., Krafft, G. A., Mamun, M. A., Palacios-Serrano, G., Poelker, M., Suleiman, R., & Zhang, S. (2019). Simulation study of the emittance measurements in magnetized electron beam. In M. Boland, H. Tanaka, D. Button, R. Dowd, & V.R.W. Schaa (Eds.), *Proceedings of the 10th International Particle Accelerator Conference* (pp. 822-825). JACoW. https://doi.org/10.18429/JACoW-IPAC2019-MOPRB110

ISBN: 978-3-95450-208-0 doi:10.18429/JACoW-IPAC2019-MOPRB110

SIMULATION STUDY OF THE EMITTANCE MEASUREMENTS IN MAGNETIZED ELECTRON BEAM*

S.A.K. Wijethunga†[1], M.A. Mamun[2], F.E. Hannon[2], G.A. Krafft[1,2], J. Benesch[2], S. Zhang[2,]
G. Palacios-Serrano[1,2], R. Suleiman[2], M. Poelker[2], J.R. Delayen[1]
[1]Old Dominion University, Norfolk, VA 23529, USA
[2]Thomas Jefferson National Accelerator Facility, Newport News, VA 23606, USA

Abstract

Electron cooling of the ion beam is key to obtaining the required high luminosity of proposed electron-ion colliders. For the Jefferson Lab Electron Ion Collider, the expected luminosity of 10^{34} $cm^{-2}s^{-1}$ will be achieved through so-called "magnetized electron cooling", where the cooling process occurs inside a solenoid field, which will be part of the collider ring and facilitated using a circulator ring and Energy Recovery Linac (ERL). As an initial step, we generated magnetized electron beam using a new compact DC high voltage photogun biased at -300 kV employing an alkali-antimonide photocathode. This contribution presents the characterization of the magnetized electron beam (emittance variations with the magnetic field strength for different laser spot sizes) and a comparison to GPT simulations.

INTRODUCTION

The proposed Jefferson Lab Electron Ion Collider (JLEIC) must provide ultra-high collision luminosity (10^{34} $cm^{-2}s^{-1}$) to achieve the promised physics goals and this necessitates small transverse emittance at the colliding position. Emittance growth can be reduced by the process called electron cooling, where the electron beam with temperature *Te* is co-propagated with the ion beam traveling at the same velocity but with temperature *Ti* where *Te* < *Ti*. The ion beam is "cooled" as a result of the Coulomb collisions and the transfer of thermal energy from ions to the electrons. Thermal equilibrium is reached when both the particles have the same transverse momentum.

The cooling rate can be significantly improved using a "magnetized electron beam" where this process occurs inside a solenoid field which forces electrons to travel with small helical trajectories that help to increase the electron-ion interaction time while suppressing the electron-ion recombination [1, 2]. However, the fringe radial magnetic field at the entrance of the solenoid creates a large additional rotational motion which adversely affects the cooling process inside the solenoid. In order to overcome this effect, the electron beam is created inside a similar field but providing a rotating motion in the opposite direction, so that the fringe field effects exactly cancel.

* Authored by Jefferson Science Associates, LLC under U.S. DOE Contract No. DE-AC05-06OR23177. Additional support comes from Laboratory Directed Research and Development program. The U.S. Government retains a non-exclusive, paid-up, irrevocable, world-wide license to publish or reproduce this manuscript for U.S. Government purposes.
† wwije001@odu.edu

The generation and characterization of the magnetized electron beam was successfully conducted at Jefferson Lab using a new DC high voltage photogun biased at -300 kV and employing a K_2CsSb photocathode. Simulations were performed using GPT (General Particle Tracer) program to benchmark the measurements. This paper presents simulations results of the emittance measurements which help to understand the theory, both qualitatively and quantitatively and to optimize the parameters for better results.

EXPERIMENTAL SETUP

The experimental beamline consists of gun high voltage chamber, bialkali-antimonide photocathode deposition chamber, cathode solenoid, 532 nm RF-pulsed laser, three fluorescent YAG screens, harp, few focusing solenoids and beam dump. A schematic diagram of the beamline is shown in Fig. 1.

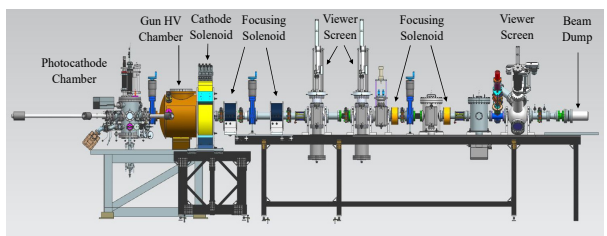

Figure 1: The diagnostic beamline.

The compact gun high voltage chamber includes an inverted insulator and spherical cathode electrode operating at or below -300 kV. The cathode-anode gap is 0.09 m and the anode aperture is 0.02 m. To manufacture photocathodes, a load-lock type photocathode deposition chamber was installed behind the gun high voltage chamber. A 532 nm green light RF-pulsed drive laser with 374 MHz bunch repetition rate and 50 ps FWHM pulse width was used for all measurements. The laser beam temporal and spatial profiles were Gaussian and the laser spot size at the photocathode was adjusted using an optical transport system with focusing lenses. The magnetic field at the photocathode was provided by a solenoid magnet designed to fit at the front of the gun chamber, 0.2 m away from the cathode. The magnet operates at a maximum current of 400 A to provide up to 0.1514 T at the photocathode. The diagnostic beam line extends 4.5 m from the photocathode with nominal 0.065 m beampipe aperture. There are two fluorescent YAG screen-slit combinations at 1.5 and 2.0 m, and one YAG screen at 3.75 m to measure the beam's transverse

ISBN: 978-3-95450-208-0 doi:10.18429/JACoW-IPAC2019-MOPRB110

density profile, and to trace the beam rotation angles. Additionally, there are four focusing solenoids at 0.49, 1.01, 2.35 and 2.94 m and several steering dipole magnets [3].

THEORETICAL BACKGROUND

The transverse emittance associated with the magnetized beam is given by [4],

$$\varepsilon_{tot} = \sqrt{{\varepsilon_u}^2 + {\varepsilon_d}^2} \quad (1)$$

where ε_u is the uncorrelated emittance combining the effect of thermal, space charge components and ε_d is the drift emittance (correlated emittance) which represents the magnetization,

$$\varepsilon_d = \frac{eB_0\sigma^2}{8m_e c} \quad (2)$$

where c is the speed of light. For efficient cooling, uncorrelated emittance should be small inside the cooling solenoid as the temperature of the electron beam is determined by the ε_u. Drift emittance is related to the beam size during transport and thus, larger drift emittance helps to reduce the collective effects such as space charge blowup.

In order to cancel the effect of the fringe radial magnetic field at the entrance of the cooling solenoid from the fringe radial magnetic field at the exit of the cathode solenoid $B_0\sigma^2$combination (drift emittance) should be chosen such that

$$B_0\sigma^2 = B_{cool}{\sigma_e}^2 \quad (3)$$

where B_{cool} and σ_e are the field and beam size inside the cooling solenoid, respectively.

EXPERIMENTAL METHOD

The solenoid scan technique was used to investigate the drift emittance variation as a function of applied cathode magnetic field. The first two focusing solenoids were used to center the electron beam on the 3rd solenoid and then the current of the 3rd solenoid was varied while measuring beam size on the 3rd viewer. This was repeated for different cathode solenoid currents (0-400 A), for three different laser spot sizes (0.23, 0.44 and 0.90× 10^{-3} m), and for -200 and -300 kV gun bias voltages. The parabolic fit to the data (the square of the beam size vs the square of solenoid current) provide a measure of the transverse beam emittance. The space charge effect was neglected because the average beam current was only a few nanoamperes.

SIMULATIONS

GPT software was used to model the beamline and compare with the measurements [5]. A 3D electric field map of the photogun anode-cathode gap that was generated using CST software, and a 2D magnetic field map of the cathode solenoid obtained using Opera were used in the simulations. The axial and transverse electric fields of the photogun are shown in Fig. 2 for the photogun biased at -300kV.

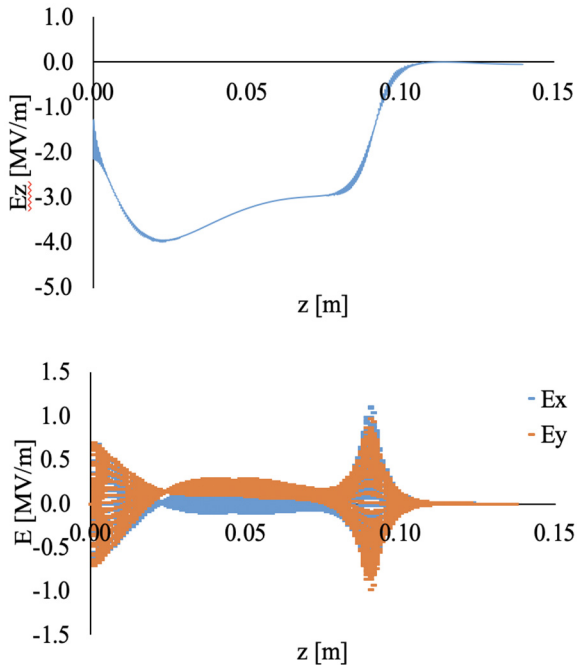

Figure 2: (top) Axial and (bottom) transverse electric field maps.

Ideally, the transverse fields should be axially symmetric throughout the anode-cathode gap. But as shown in Fig. 2 E_y is not symmetric along the axis due to the photogun geometry and this results in a vertical deflection of the beam as it leaves the photogun. Steering magnets near the photogun were used to put the beam on axis. Similarly, the GPT optimizer program was used to adjust steering magnet settings near the photogun to put the beam on axis throughout the beamline.

The axial magnetic field of the cathode solenoid is shown in Fig.3, for the cathode solenoid set to 400 A and with the beamline focusing solenoids set at maximum values. We found that the magnetic field was distorted by the steel field clamps of the focusing solenoids as shown in Fig. 3. In order to make the beam smaller throughout the beamline and match the measurement conditions, the first two focusing solenoids were used in the simulations.

The GPT RMS emittance routines, "nemixrms" and "nemiyrms" were used to obtain the total transverse emittance variations along the beamline and "nemirrms" was used to obtain the uncorrelated emittance variations along the beamline which removes the r-p_phi coupling due to the solenoid field from the normalized emittance calculation.

ISBN: 978-3-95450-208-0 doi:10.18429/JACoW-IPAC2019-MOPRB110

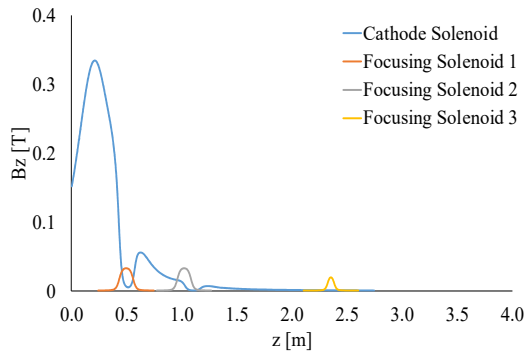

Figure 3: The magnetic field map of the cathode solenoid and first three focusing solenoids fields.

The starting condition input parameters used for the simulations are shown in Table 1.

Table 1: Input Parameters Used in Simulations

Parameter	Value
Maximum gun high voltage [kV]	-300
Max magnetic field, B_z at the cathode [T]	0.1514
Mean Transverse Energy [eV]	0.130
Pulse width, Gaussian (FWHM) [ps]	50
Transverse laser spot size, Gaussian (rms) [mm]	0.23,0.44, 0.90
Bunch charge [pC]	1
Horizontal offset of the laser [mm]	0
Vertical offset of the laser [mm]	1.7

SIMULATION RESULTS ANALYSIS

The following plots compare the measurements and GPT simulations. Figure 4 shows the drift emittance variations with the cathode solenoid field for different laser spot sizes.

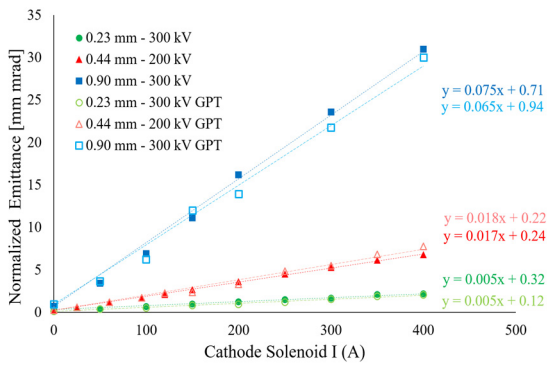

Figure 4: Drift emittance variations with the cathode solenoid field for different laser spot sizes.

There is a clear linear dependence of the drift emittance on the applied cathode magnetic field, which is consistent with Eq. (2). In addition, there is good agreement between measurements and simulations. We observed significant beam loss for high magnetic field strengths, and this made it difficult to measure accurately the desired drift emittance of 36 mm mrad for 0.1514 T field at the cathode and 0.9 × 10^{-3} m laser spot size. This observation also speaks to future challengers of transporting beam with high magnetization at the JLEIC cooler.

Figure 5 shows GPT results of the drift (top) and uncorrelated (bottom) emittance variations along the beamline. The drift emittance plot shows huge emittance variation from 0-2.5 m which is the region of the cathode solenoid field and 1st two focusing solenoid fields. The reason is the beam rotation around the z axis and thus the resulting strong r-p_phi correlations. This is just an artifact of the numerical method used to calculate the emittance. When the solenoid field vanishes, emittance decreases and returns back to a constant value as shown from 2.5-4 m. For the uncorrelated emittance, when all the correlations are removed emittance should be small and a constant throughout the beamline. But we see a small bump near z= 0.5-1 m as a result of the distorted magnetic field between the region.

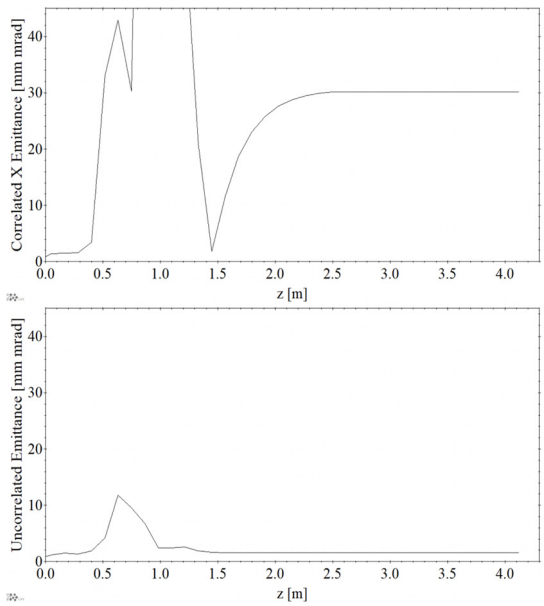

Figure 5: (top) Drift emittance for 0.1514 T field at the cathode and 0.9 × 10^{-3} m laser spot size. (bottom) Uncorrelated emittance same conditions.

As predicted by theory, correlated emittance is clearly larger than the uncorrelated emittance which is seen by the ion beam inside the cooling solenoid and helps to increase the cooling efficiency.

CONCLUSION

In summary the magnetized electron beam generated at JLab was successfully modelled using GPT software. In order to evaluate the magnetization, normalized transverse emittance measurements were performed as a function of cathode magnetic field strength for different laser spot sizes. Simulations show a good agreement with the measurements and the clear difference between the correlated and uncorrelated emittances.

ISBN: 978-3-95450-208-0 doi:10.18429/JACoW-IPAC2019-MOPRB110

ACKNOWLEDGMENTS

This work is supported by the Department of Energy, under contract DE-AC05-06OR23177 and the Laboratory Directed Research and Development program.

REFERENCES

[1] Ya. Derbenev and A. Skrinsky, "Magnetization effect in electron cooling," *Fiz.Plazmy*, vol. 4, 492, 1978; [Sov.J. Plasma Phys. **4**, 273 (1978)].

[2] R. Brinkmann, Y. Derbenev and K. Flöttmann, "A low emittance flat-beam electron source for linear colliders," *Phy. Rev. ST Accel.Beams*, vol. 4, p. 053501, 2001.

[3] M.A. Mamun *et al.*, "Production of magnetized electron beam from a DC high voltage photogun", in *Proc. 9th Int. Particle Accelerator Conf. (IPAC'18)*, Vancouver, BC, Canada.

[4] K.-J. Kim, *Phys. Rev. ST Accel. Beams* 6, 104002, (2003).

[5] S.B. van der Geer and M.J. de Loos, "General Particle Tracer" user manual.